

Optimal Occulter Design for Finding Extrasolar Planets

Robert J. Vanderbei

Operations Research and Financial Engineering, Princeton University

rvdb@princeton.edu

Eric Cady

Mechanical and Aerospace Engineering, Princeton University

ecady@princeton.edu

and

N. Jeremy Kasdin

Mechanical and Aerospace Engineering, Princeton University

jkasdin@princeton.edu

ABSTRACT

One proposed method for finding terrestrial planets around nearby stars is to use two spacecraft—a telescope and a specially shaped occulter, whose shape is specially designed to prevent all but a tiny fraction of the starlight from diffracting into the telescope. As the cost and observing cadence for such a mission will be driven largely by the separation between the two spacecraft, it is critically important to design an occulter that can meet the observing goals while flying as close to the telescope as possible. In this paper we explore this tradeoff between separation and occulter diameter. More specifically, we present a method for designing the shape of the outer edge of an occulter that is as small as possible and gives a shadow that is deep enough and large enough for a 4m telescope to survey the habitable zones of many stars for Earth-like planets. In particular, we show that in order for a 4m telescope to detect in broadband visible light a planet 0.06 arcseconds from a star shining 10^{10} times brighter than the planet requires a specially-shaped occulter 50m in diameter positioned about 72,000 km in front of the telescope.

Subject headings: Extrasolar planets, occulter, apodization, petal-shaped mask, Babinet's principle

1. Introduction

Since the first extrasolar planet was discovered by Mayor and Queloz (1995), various techniques have been used to infer the presence of large planets, but none have the capability to image Earth-like planets directly. Finding terrestrial planets is difficult because the difference in brightness between the star and the planet is so large; in the visible spectrum, the intensity difference, or contrast, is approximately 10^{10} (see Marais et al. (2002)). Just as importantly, the angular separation between planet and star is on the order of 0.1 arcseconds for a star 10 parsecs from Earth. The problem becomes one of reducing the intensity of starlight at the planet’s location by a factor of 10^{10} . Several methods (see Kasdin et al. (2003); Kuchner and Traub (2002); Vanderbei (2006); Guyon (2003)) have been proposed to do this within the telescope by adjusting the point spread function so that there is very little starlight at the location of the planet in the image plane of the telescope. While these techniques have demonstrated the potential to provide the necessary contrast (Sidick et al. (2006)), they have the intrinsic difficulty that they require an adaptive-optics system within the telescope to correct aberrations in the wavefront (induced largely by imperfect optics), which tend to spill unwanted light into the search area.

One solution to this problem is to remove the starlight before it reaches the telescope by using a second spacecraft, an *occulter*, positioned between the telescope and the target star. Such a concept was first proposed by Spitzer (1962); since then, a number of proposals (see Copi and Starkman (2000); Schultz et al. (2003); Cash (2006)) have appeared that use occulters to look for planets, both of Jupiter and Earth size.

Ray optics predicts that the physical shape of the occulter blocks the light from the star while allowing the light of a nearby planet to pass by the edge. A telescope would then be able to see everything in the system at once, up to the edge of the disk. Everything behind the disk, including the entire star, would be stopped by the opaque occulter. Unfortunately, this analysis neglects diffraction, which is a significant factor in propagations involving such narrow angles. It was known as early as 1818 that diffraction around objects could produce light in areas that geometric optics would predict to be dark; the notable example of this is Poisson’s spot, which earned Fresnel a prize from the French Academy of Sciences (see Goodman (1996)). A proper design of an occulter-based mission thus requires careful consideration of these diffraction effects.

Spitzer (1962) noted that it was sufficient to change the transmission function with radius in order to suppress this central spot. Subsequent papers have suggested some specific mechanisms for accomplishing this. One concept, called the *Big Occulting Steerable Satellite (BOSS)* (Copi and Starkman (2000)), is based on a transmissive apodization defined by polynomials. A more recent entry into this field is the *New Worlds Observer* proposed

by Webster Cash and funded by NIAC. Originally conceived as a pinhole camera in space (Simmons et al. (2004)), it was eventually reincarnated as a space-based occulter (Simmons (2005); Cash (2006)). The proposed New Worlds Observer mission has generated much excitement recently in the planet-finding community. The purpose of this paper is to explore some of the design trade-offs one will likely have to face in deciding on the best design to push forward.

2. Babinet’s principle

An occulter is complementary to a pinhole camera; instead of allowing light only through a small hole, an occulter allows all light except for the light blocked by the occulter which now replaces the small hole. This complementarity allows us to calculate the downstream electric field produced by an occulter using Babinet’s principle; that is, the sum of the light passing around the occulter and the light passing through an occulter-shaped hole is a free-space plane wave. The electric field past the occulter is thus given by

$$E_o = E_u - E_h \tag{1}$$

where E_o is the field due to the occulter, E_u is the unobstructed field, and E_h is the field due to the hole. From the Helmholtz equation it follows that a plane wave having complex amplitude E_0 at the plane of the occulter will be given by $E(\rho, \phi) = E_0 e^{2\pi i z / \lambda}$ at the telescope’s pupil plane, which is located a distance z behind the occulter. Here, and throughout the paper, we use polar coordinates (ρ, ϕ) to represent the pupil plane of the telescope. We assume that $\rho = 0$ corresponds to the center of the pupil.

Before we investigate simple shaped occulters, it is instructive to consider a more general setting in which an occulter (or a hole) need not be purely opaque or transparent. Instead, we introduce the possibility for partial attenuation. To this end, we introduce a function $A(r, \theta)$ to denote the attenuation profile for the occulter (we use r and θ to denote polar coordinates in the plane of the occulter). If $A(r, \theta)$ takes the value 1 somewhere, then no light gets through at that point. On the other hand, if it takes the value zero, then all light gets through. All values in between are allowed. Under circular symmetry, the attenuation profile $A(r, \theta)$ does not depend on θ and so we can write $A(r)$ for the attenuation profile. Of course, when thinking about transmission through a “tinted” hole, the function $A(r)$ represents the level of transmission rather than attenuation. That is, $A(r)$ describes an apodization of the hole. With these assumptions, E_h at the occulter plane can be written as

$$E_h(r) = E_u A(r) = E_0 A(r). \tag{2}$$

Assuming that the function $A(r)$ is zero for r larger than some threshold R , the Fresnel integral for the propagation of the field from the hole a distance z can then be written in polar coordinates (Goodman (1996)) as

$$E_h(\rho) = E_0 \frac{2\pi}{i\lambda z} e^{\frac{2\pi iz}{\lambda}} e^{\frac{\pi i \rho^2}{\lambda z}} \int_0^R J_0\left(\frac{2\pi r \rho}{\lambda z}\right) A(r) e^{\frac{\pi i}{\lambda z} r^2} r dr \quad (3)$$

and the field due to an occulter can be expressed as

$$E_o(\rho) = E_0 e^{\frac{2\pi iz}{\lambda}} \left(1 - \frac{2\pi e^{\frac{\pi i \rho^2}{\lambda z}}}{i\lambda z} \int_0^R J_0\left(\frac{2\pi r \rho}{\lambda z}\right) A(r) e^{\frac{\pi i}{\lambda z} r^2} r dr \right). \quad (4)$$

3. Optimal attenuation functions

We find $A(r)$ by minimizing the “extent” of $A(r)$ subject to the constraint that the intensity, which is the square of the magnitude of the electric field, in a specified dark region is no more than 10^{-10} . To be precise, we

$$\begin{aligned} & \text{minimize} && \int_0^R A(r) r dr \\ & \text{subject to} && |E_o(\rho)|^2 \leq 10^{-10} |E_0|^2, \quad 0 \leq \rho \leq \rho_{\max} \\ & && 0 \leq A(r) \leq 1, \quad 0 \leq r \leq R. \end{aligned} \quad (5)$$

This is an infinite-dimensional, quadratic programming problem, which would produce a shadow from 0 to ρ_{\max} with 10^{10} contrast at the telescope’s pupil plane. Unfortunately, it is computationally intractable. To make it solvable, we introduce certain simplifications to reduce it to a finite-dimensional, linear programming problem.

First, we rewrite the constraint on $E_o(\rho)$ as:

$$|E_o(\rho)| \leq 10^{-5} |E_0| \quad (6)$$

Since $E_o(\rho)$ is complex, we can constrain the magnitude of the real and imaginary parts of $E_o(\rho)$ to be less than or equal to $10^{-5} |E_0| / \sqrt{2}$ to get a more conservative, but linear, constraint on $E_o(\rho)$. Finally, we discretize $[0, R]$ and $[0, \rho_{\max}]$ to get a finite-dimensional program.

As formulated, this problem would only produce the desired shadow at the single selected wavelength. For broadband observations, we make a simple extension to this approach and define the optimization to provide a sufficient shadow at multiple wavelengths. For this, the constraints are repeated for each wavelength for which a shadow is desired; the depth of the

shadow can be changed by replacing 10^{-5} with a new constraint, and the width by allowing ρ_{\max} to vary with λ .

Practical considerations also provide further constraints. For a realistic binary occulter, the innermost section should be opaque out to some radius a to accommodate the spacecraft. This is expressed as:

$$A(r) = 1, \quad 0 \leq r \leq a \quad (7)$$

We might also wish the petals to get thinner as they unfold outward, which requires $A'(r) \leq 0$, or for the profile to be smooth, which requires $|A''(r)|$ to be bounded by some value.

4. Adding petals

Unfortunately, it is not currently possible to build an apodized occulter to the required precision. So, instead, replace the apodized occulter with a binary occulter of a particular shape. For instance, inspired by Vanderbei et al. (2003), Cash (2006) suggested using an occulter made up of a set of N identical evenly spaced “petals” as shown in Figure 1. These petals are wedges of the circle whose width varies with radius such that the fractional angular extent of the occulter at a given radius is the attenuation profile $A(r)$. Except for Babinet’s principle, this petal-shaped occulter is identical to the starshaped pupil masks described in Vanderbei et al. (2003). The resulting propagated field for such an occulter is thus found via the same procedure using the Jacobi-Anger expansion. The result is

$$\begin{aligned} E_{o,\text{petal}}(\rho, \phi) &= E_{o,\text{apod}}(\rho) \\ &- E_0 e^{\frac{2\pi iz}{\lambda}} \sum_{j=1}^{\infty} \frac{2\pi(-1)^j}{i\lambda z} \left(\int_0^R e^{\frac{\pi i}{\lambda z}(r^2 + \rho^2)} J_{jN} \left(\frac{2\pi r \rho}{\lambda z} \right) \frac{\sin(j\pi A(r))}{j\pi} r dr \right) \\ &\times (2 \cos(jN(\phi - \pi/2))) \end{aligned} \quad (8)$$

where $E_{o,\text{apod}}(\rho, z)$ is the field from the smooth apodization and N is the number of petals (assumed even). For large N , all of the J_{jN} ($j > 0$) become small exponentially fast near the center of the telescope and so the field approaches that of the smooth apodization as N increases.

5. Results

One consideration that must be taken into account when designing optimized occulters is angular size of the shade. As mentioned in Sec. 1, the maximum angular separation

between Earth-like planets and their stars is 0.1 arcsecond for a star 10 parsecs distant. The angular size of the shade is R/z . For example, for a 25 m radius shade, the shade must be at least 51600 km distant. If we want to see planets at smaller angular separations, i.e., further from Earth, the shade must be shrunk or the distance increased. We present a series of shades optimized with different sizes and at different distances.

Radially-symmetric apodizations were created to provide 10^{10} contrast out to a given radius for four separate occulter profiles:

- 18m occulter, 18000 km distance, 3m shadow radius
- 20m occulter, 36000 km distance, 3m shadow radius
- 25m occulter, 72000 km distance, 2.5m shadow radius
- 30m occulter, 100000 km distance, 2.5m shadow radius

These occulters were designed to provide the specified contrast over a band from 400nm to 1100nm. The radial profiles of the shadow at the telescope are shown in Fig. 2.

Once a profile is created by optimization, we use Eq. 8 to calculate the effect of converting a smooth apodization to petals; this petalization tends to reduce the width of the shadow at certain angles. In a forthcoming paper, we will present a method of optimizing the petal shape directly, to prevent this degradation. Each of the four occulters was converted to a binary occulter with 16 petals; the performance of these occulters at 400nm, 700nm, and 1100nm is shown in Fig. 3.

Finally, some may suggest that it is overly conservative to insist on 10^{10} contrast at the telescope’s pupil plane since additional contrast is generated by the telescope itself as it forms an image. The residual starlight, being roughly flat across the telescope’s pupil, forms something similar to an Airy pattern in the image plane. The planet will be slightly off-axis and therefore offset slightly from the on-axis Airy pattern. Since the first diffraction ring in an Airy pattern is almost two orders of magnitude suppressed relative to its main lobe, one can expect some benefit. To test this, we modified our optimization code to minimize an upper bound on the intensity of the light over a 6m diameter shadow. We ran tests assuming various separations z . The tip radius R was fixed so that the a planet appearing at the tip is 0.060 arcseconds off-axis (i.e., we set R/z radians equal to 60 milliarcseconds and solved for R). The smallest value of z that provides a sufficiently dark hole for the planet to be detectable in the image plane turns out to be 66000km. For this case, the shadow at the telescope’s pupil is slightly brighter than 10^{-8} times the unattenuated brightness. In the image plane, a planet at 60 milliarcseconds has about the same brightness as the residual starlight falling in the same location in the image (a $Q = 1$ detection in TPF parlance).

Figure 4 shows image plane images for the 66000km design described here. Also shown in the figure for comparison is the image plane image for the 72000km design described earlier.

6. Final Remarks

One thing that should not be separated from occulter edge design is systems engineering. Occulters close to the telescope take less fuel to hold in place, but must be smaller than occulters further out, and in the past these smaller shades have often proved difficult to optimize without losing science capability in the process. Shades that are too large would simply blot out a close-in planet. Shades further away from the telescope can be larger, but the orbits are more costly to maintain, and limits on fuel can constrain the number of stars that can be visited. Moreover, larger occulters may prove more vulnerable to deformation and damage.

Decreasing the number of petals decreases the quantity of the equipment required to unfold them, reducing both mass and risk for the occulter. It also tends to reduce the total perimeter of the occulter, bringing down the amount of light scattered off the edges. However, petalizing causes the edges of the shadow to encroach inward, and the edges move in further as petal number shrinks. This in turn requires tighter tolerances on attitude and position for both the shade and telescope, increasing the requirements on the control systems. For this reason, it is useful to be able to develop feasible designs at a variety of shade sizes and distances, in order for the engineering tradeoffs to be accommodated.

The authors would like to thank R. Lyon for a number of fruitful discussions. We acknowledge support from the Goddard Space Flight Center and Sigma Space Corporation, contract #NNG06EE69C. R. Vanderbei acknowledges support from the ONR (N00014-05-1-0206).

REFERENCES

- W. Cash. Detection of earth-like planets around nearby stars using a petal-shaped occulter. *Nature*, 442:51–53, 2006.
- C.J. Copi and G.D. Starkman. The *Big Occulting Steerable Satellite* [BOSS]. *Astrophysical Journal*, 532:581–592, 2000.
- J.W. Goodman. *Introduction to Fourier Optics*. McGraw-Hill, 1996.

- O. Guyon. Phase-induced amplitude apodization of telescope pupils for extrasolar terrestrial planet imaging. *Astronomy & Astrophysics*, 404:379–387, 2003.
- N.J. Kasdin, R.J. Vanderbei, D.N. Spergel, and M.G. Littman. Extrasolar planet finding via optimal apodized pupil and shaped pupil coronagraphs. *Astrophysical Journal*, 582: 1147–1161, 2003.
- M.J. Kuchner and W.A. Traub. A coronagraph with a band-limited mask for finding terrestrial planets. *Astrophysical Journal*, 570:900–908, 2002.
- D.J. Des Marais, M.O. Harwit, K.W. Jucks, J.F. Kasting, D.N. Lin, J.I. Lunine, J. Schneider, S. Seager, W.A. Traub, and N.J. Woolf. Remote sensing of planetary properties and biosignatures on extrasolar terrestrial planets. *Astrobiology*, 2(2):153–181, 2002.
- M. Mayor and D. Queloz. A jupiter-mass companion to a solar-type star. *Nature*, 378: 355–359, 1995.
- A.B. Schultz, I.J.E. Jordan, M. Kochte, D. Fraquelli, F. Bruhweiler, J.M. Hollis, K.G. Carpenter, R.G. Lyon, M. DiSanti, C. Miskey, J. Leitner, R.D. Burns, S.R. Starin, M. Rodrigue, M.S. Fadali, D. Skelton, H.M. Hart, F. Hamilton, and K.-P. Cheng. UMBRAS: A matched occulter and telescope for imaging extrasolar planets. In *Proceedings of SPIE–High-Contrast Imaging for Exo-Planet Detection*, volume 4860, 2003.
- E. Sidick, F. Shi, S. Basinger, D. Moody, A.E. Lowman, A.C. Kuhnert, and J.T. Trauger. Performance of TPF’s high-contrast imaging testbed: modeling and simulations. In *Proceedings of SPIE–Space Telescopes and Instrumentation I: Optical, Infrared, and Millimeter*, volume 6265, 2006.
- W. L. Simmons, W. C. Cash, S. Seager, E. Wilkinson, N. J. Kasdin, R. J. Vanderbei, N. Chow, E. Gralla, and J. Kleingeld. The New Worlds Observer: a mission for high-resolution spectroscopy of extra-solar terrestrial planets. In *Microwave and Terahertz Photonics. Edited by Stohr, Andreas; Jager, Dieter; Iezekiel, Stavros. Proceedings of the SPIE, Volume 5487, pp. 1634-1645 (2004).*, pages 1634–1645, October 2004. doi: 10.1117/12.552069.
- W.L. Simmons. A pinspeck camera for exo-planet spectroscopy. Technical report, M.S. Thesis, Department of Mechanical and Aerospace Engineering, Princeton University, 2005.
- L. Spitzer. The beginnings and future of space astronomy. *American Scientist*, 50:473–484, 1962.

- R.J. Vanderbei. Diffraction analysis of two-dimensional pupil mapping for high contrast imaging. *Astrophysical Journal*, 636:528–543, 2006.
- R.J. Vanderbei, D. Spergel, and N.J. Kasdin. Circularly symmetric apodization via star-shaped masks. *Astrophysical Journal*, 599:686–694, 2003.

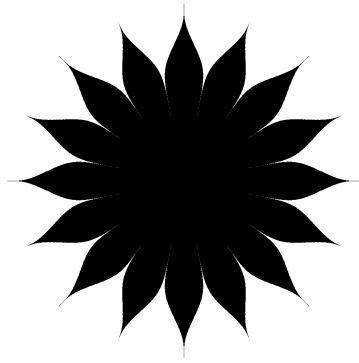


Fig. 1.— An optimally-shaped sixteen-petal occulter.

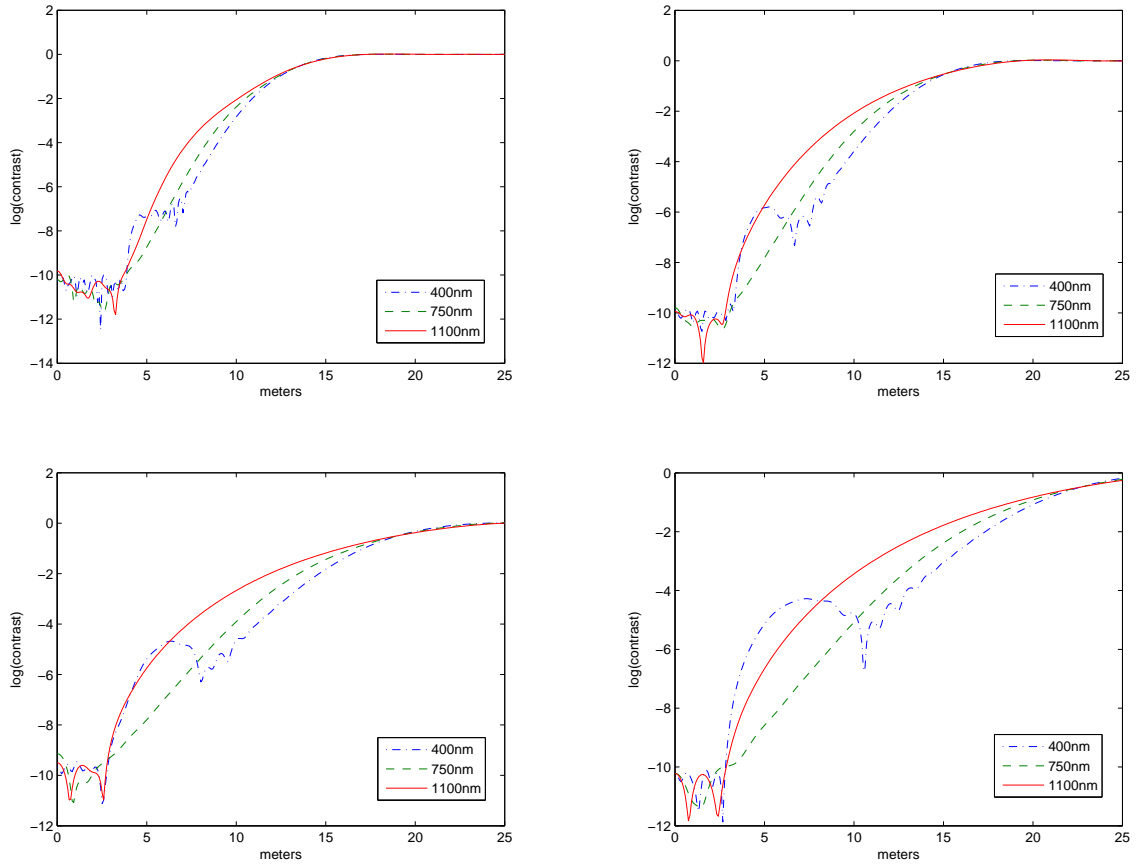


Fig. 2.— These plots show the radial profile of the shadow at the telescope, in different wavelengths. *Top left.* This plot is for an 18m occulter at 18000km. *Top right.* This plot is for a 20m occulter at 36000km. *Bottom left.* This plot is for an 25m occulter at 72000km. *Bottom right.* This plot is for a 30m occulter at 100000km.

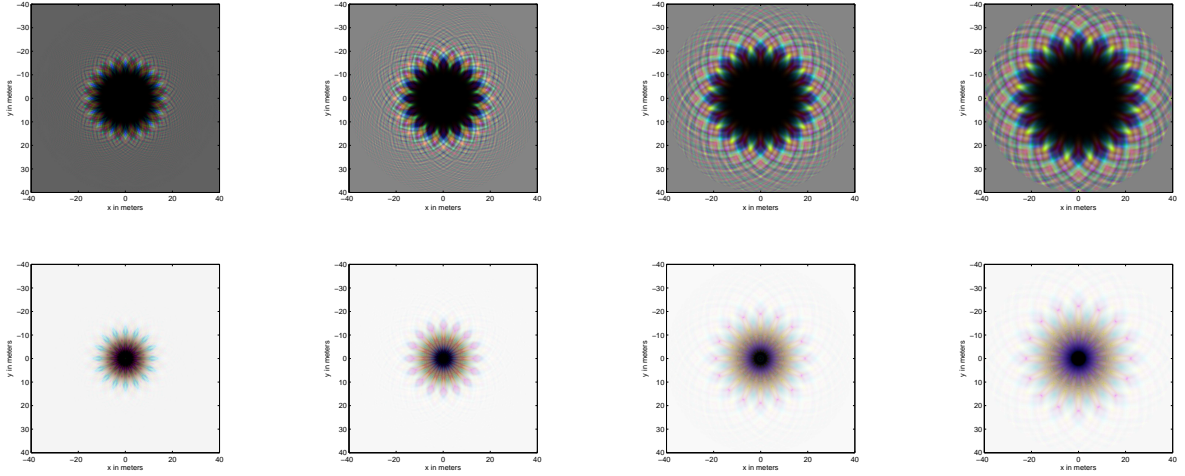


Fig. 3.— The shadow cast at the telescope pupil plane for four different occulter distances, which are from left to right 18,000km, 36,000km, 72,000km, and 100,000km. The top row shows linear stretch plots whereas the bottom row shows logarithmic stretches with 10^{-10} set to black. These are RGB images composited using $\lambda = 1.0\mu\text{m}$ for the red channel, $\lambda = 0.7\mu\text{m}$ for the green channel, and $0.4\mu\text{m}$ for the blue channel.



Fig. 4.— These plots are simulated (noiseless) images at the telescope’s image plane. The RGB images were computed using $\lambda = 1.0\mu\text{m}$ for the red channel, $\lambda = 0.7\mu\text{m}$ for the green channel, and $0.4\mu\text{m}$ for the blue channel. In both images, the off-axis planet is positioned at the tip of the the occulter. *Left.* This image is for an $R = 22\text{m}$ occulter at 66000km. The planet shown here is at 60 milliarcseconds. *Right.* This plot is for an $R = 25\text{m}$ occulter at 72000km. The planet shown here is at 72 milliarcseconds.